A micromechanical investigation of sand–rubber mixtures using the discrete element method

Ru Fu[1], Bo Yang[2], Xinli Hu[1], Bo Zhou[2]* and Matthew Richard Coop[3]

[1]Faculty of Engineering
China University of Geosciences
Wuhan, China

[2]School of Civil and Hydraulic Engineering
Huazhong University of Science and Technology
Wuhan, China

[3]Department of Civil, Environmental and Geomatic Engineering
University College London
London, United Kingdom

* Corresponding authors:
Dr. Bo Zhou, zhoubohust@hust.edu.cn

Abstract

Mixing soil or sand with tire rubber fibers or buffings is a practical and promising solution to the problem of global scrap tire pollution. However, sand–rubber mixtures exhibit unsatisfactory and complex mechanical properties in engineering applications due to the large deformation of rubber fibers. In this study, a detailed numerical approach to modeling mixtures of sand and rubber fibers via the discrete element method (DEM) was proposed, and the effect of rubber content on the macroscopic and microscopic mechanical behaviors of sand–rubber mixtures was investigated. Furthermore, the reinforcing mechanism by which rubber fibers contribute to the micromechanics of sand–rubber mixtures was explored to determine the optimum rubber content in terms of soil mechanical performance. Comparative analysis of the experimental and numerical results demonstrated the applicability and ability of the proposed DEM model and related parameters for modeling sand–rubber mixtures. Through investigation of the constitutive behaviors of sand–rubber mixtures with various rubber contents under triaxial compression, a rubber content of 20% was found to provide the best shear resistance in the critical state. The micromechanics of sand–rubber mixtures, namely particle kinematics, the interparticle coordination number and rubber fiber deformation, were investigated to demonstrate the specific reinforcing mechanism of rubber fibers with respect to improved soil performance. The resulting data strongly support the identified optimum rubber content for sand–rubber mixtures that will provide a valuable guidance to the relevant engineering applications.

Keywords: Sand–rubber mixture; Discrete element method; Local shear band; Coordination number; Rubber fiber deformation

1 Introduction

Environmental protection and construction material resource are important issues in engineering geological fields. The development of the automotive industry has led to the accumulation of an alarming volume of scrap tires worldwide. Most of these waste tires are discarded in landfills or tire stockpiles, leading to serious environmental problems (Kawata et al., 2008). Accordingly, there is an urgent global need for green and economical scrap tire recycling options, such as the use of waste tire rubber-derived products as construction materials in geotechnical and geological engineering applications.

Due to advantages such as light weight, low cost and easy processing, rubber-derived products are used widely as subgrade and embankment fillings (Yoon et al., 2006; Edincliler et al., 2010; Soleimanbeigi and Edil, 2015); to reinforce weak soil foundations (Humphrey, 2007; Moghaddas Tafreshi et al., 2013 and 2019) and retaining walls (Ahn and Cheng, 2014; Reddy and Krishna, 2015); and as alternative aggregates for light concretes (Batayneh et al., 2008; Liu et al., 2012; Thomas and Gupta, 2016). Over the last two decades, these successful applications have demonstrated the potential value of these rubber-derived products in the above mentioned geotechnical construction applications and suggested a purpose for recycled waste tires. However, as tire rubber shows large deformation, the mechanical performance (e.g., bearing capacity and deformation) of rubber fills and soil–rubber mixtures in relevant engineering applications has become a major concern (ASTM, 2008). Studies are urgently needed to investigate the mechanical properties of soil–rubber mixtures and determine the optimum rubber content in terms of mechanical performance.

According to practical engineering requirements, waste tires are usually manufactured into rubber-derived products, such as rubber chips, rubber shreds, rubber crumbs and rubber fibers, and then mixed with soils such as backfills to improve various soil properties. Through many laboratory and in-situ experiments, researchers have found that these added rubber-derived products can significantly improve the permeability, compressibility, expansibility, tensile strengths and shear strengths of clayey and expansive soils (Cetin H. et al., 2006; Trouzine, 2012; Soltani et al., 2018; Abbaspour et al., 2020). However, the effectiveness of rubber-derived products as a means of reinforcing sandy soils is still a controversial issue in research and practical engineering. Recently, Tasalloti et al. (2021) made a comprehensive literature review on the physical and mechanical properties of granulated rubber mixed with granular soils. The latest results and findings were presented and discussed primarily in terms of effects of rubber content and particle size ratio on compaction, permeability, strength and compression properties along with dynamic and cyclic deformation characteristics of sand-rubber mixtures. These experimental studies found that the addition of rubber shreds, chips and crumbs can increase slightly the critical shear strength of sand–rubber mixtures (Attom, 2006; Anbazhagan et al., 2017; Benessalah et al., 2019; Al-Rkaby, 2019). However, other studies observed the opposite result, namely a decrease in the shear resistance of the mixtures with increased rubber content, especially at the peak state (Cabalar, 2011; Noorzad and Raveshi, 2017; Balaban et al., 2019).

In light of the successful use of polypropylene fibers to improve soil properties (Consoli et al., 2002; Cheng et al., 2020a), researchers and engineers have attempted to use rubber buffings or fibers to reinforce sandy soils. According to recent publications, the addition of waste tire textile fibers to various kinds of soils can effectively improve the geotechnical properties of clayed and expansive soils, such as their tensile strength and hydraulic conductivity (Kalkan, 2013; Bekhiti et al., 2019; Narani et al., 2020), and those of sandy soils, such as their ductility, peak strength and critical shear strength (Fu et al., 2017a and 2018; Shekhawat et al., 2018).

However, tire rubber fibers are more easily deformed than the polypropylene fibers commonly used to reinforce soils. Therefore, soil–rubber mixtures have always exhibited complicated and unsatisfactory mechanical performance (Akbulut et al., 2007; Santos et al., 2010; Fu et al., 2018). In practical applications that use these mixtures, many important factors should be considered, including the stress condition, content, length and aspect ratio of the rubber fibers. Moreover, the large deformation of rubber-derived products leads to highly complex mechanisms of interaction between the rubber and soil particles, which are very difficult to explore using traditional experiments or in-situ testing.

As an alternative, the discrete element method (DEM) has become a powerful tool to investigate the fundamental micromechanics of granular materials over the past four decades. Recently, the DEM has been successfully applied to simulate the behaviors of sand–rubber mixtures (Valdes and Evans, 2008; Lee et al., 2014). The numerical predictions of mechanical behaviors presented consistent trends with the experiments, and further provided a full access to the particle-scale information (e.g., particle kinematics and interparticle contact forces) within sample deformation. By using DEM, Lopera Perez et al. (2016) investigated the effect of rubber size on the behaviors of sand-rubber mixtures, and revealed the micromechanics underlying the sand-rubber interaction in terms of coordination number, structural anisotropy, contribution of contact type and contact force network. The same authors further extended their studies on the liquefaction potential and critical state behaviors of soil-rubber mixtures at large strains (Lopera Perez et al., 2017 and 2018). However, these DEM studies were performed using simple spherical particles to simulate the behaviors of sand and rubber particles, and the pure rubber and pure sand samples were separately calibrated using data found in existing publications.

To overcome this problem, many researchers adopted the multi-sphere approach, namely clump or cluster, to simulate the stiff sand or soft rubber particles with different shapes, e.g. irregular sand grains and rubber shreds (Asadi et al., 2018a and 2018b), and realistic shapes (Asadi et al., 2021); platy rubber chips but spherical sand particles (Zhang et al., 2021); irregular gravel particles and cubic-like tire shreds (Chew et al., 2022). These DEM studies successfully revealed the effects of rubber size, type, content and stress conditions on the mechanical behaviors of sand–rubber mixtures, and further provided in-depth insights into the micromechanics of the sand–rubber interactions. By carefully reviewing these literatures, rare DEM study focused on the mixture of sand with rubber fiber. To the best of the authors' knowledge, Gong et al. (2020) were the first to simulate the mixture of sand with rubber fiber by spherical particles with rolling resistance and line-shaped clumps within DEM. However, the reinforcing mechanism of the rubber fiber on soil strength, especially for its impact on the shear banding development, was still not clear so far.

Accordingly, the objective of this study was to develop a detailed numerical method of modeling mixtures of granular soils with tire rubber fibers in DEM. We also investigated the effects of rubber content and confining pressure on the macroscopic and microscopic mechanical behaviors of sand–rubber mixtures subjected to triaxial compression. The results of real experiments and DEM simulations were initially subjected to comparative analysis to validate and calibrate the DEM and DEM parameters proposed for modeling sand–rubber mixtures. The micromechanical features of sand–rubber mixtures, specifically particle kinematics, the interparticle coordination number and rubber fiber deformation, were investigated to identify the specific mechanism by which the rubber fibers provided mechanical reinforcement. Finally, this study aimed to determine the optimum rubber fiber content in terms of the macroscopic and microscopic mechanical performance of granular soils, which will be applicable to future engineering applications.

2 Discrete element method modeling

The base sand used in this study was Leighton Buzzard sand (LBS), a standard quartz sand that deposits in shallow seas and estuarine environments. Due to its mineral composition and geological origin, the particle morphology of LBS was characterized by sub-ellipsoid form, rounded corner and smooth surface texture, as shown by Fig. 1(a). The sand sample was sieved to obtain particles in the size range of 1.18 – 2.36 mm. As demonstrated in Fig. 1(b), the rubber fibers used in this study had an average length of 11.0 mm and an approximate diameter of 1.4 mm. To determine the basic mechanical behaviors, a set of tests and a uniaxial tensile tests were conducted on a pure sand sample and rubber fibers, respectively. The results of which were also used to calibrate the microscopic parameters applied in the DEM simulations. The sand–rubber mixture samples with rubber contents of 10% and 30% were subjected to triaxial testing to validate the DEM model. All the experimental results are presented and discussed with the DEM results in the following sections.

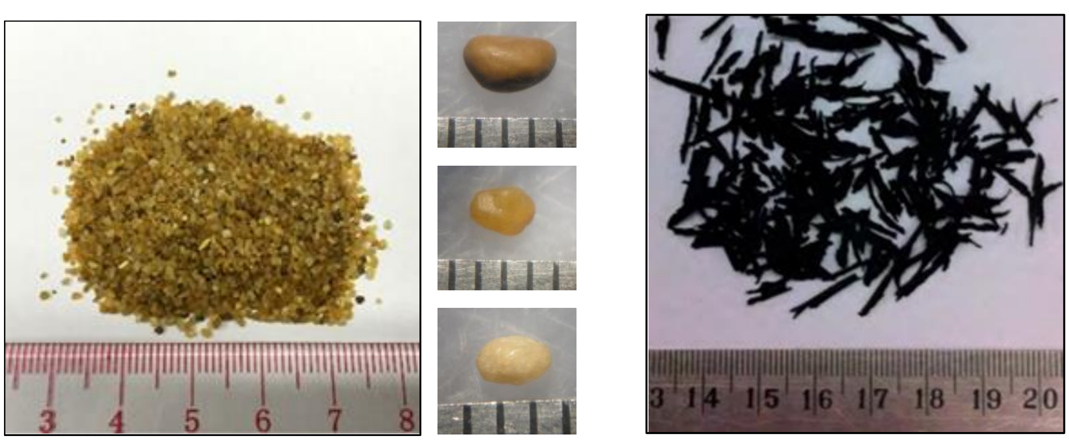

(a) (b)

Fig. 1 Photographs of the research materials: a) Leighton Buzzard sand, and b) rubber fibers

As the chosen LBS particles had sub-ellipsoid form and rounded and corners, a monotonic ellipsoid-shaped particle was established within the DEM framework using the clump logic, as demonstrated in Fig. 2(a). This particle shape was widely adopted by many DEM studies (Yang et al., 2017; Jiang et al., 2018 and Wu et al., 2020) to simulate a more realistic mechanical response of granular soils. The Clump logic can be used to generate particles with ideal shapes by bonding a small number of overlapping ball elements as rigid bodies without calculating the internal contact forces, thereby improving the computing efficiency of DEM simulations (Itasca, 2016). In contrast, as illustrated in Fig. 2(b), a cluster comprising a line of ball elements was used to model a rubber fiber. The artificial roughness of the produced rubber fiber was observed by using this modelling technique. Therefore, the friction coefficient of rubber fibers should be slightly adjusted within the calibration to compromise its influence. On account of the computation efficiency, a limitation of this study was the usage of the monotonic and simple shapes for the representation of the sand particle and rubber fiber.

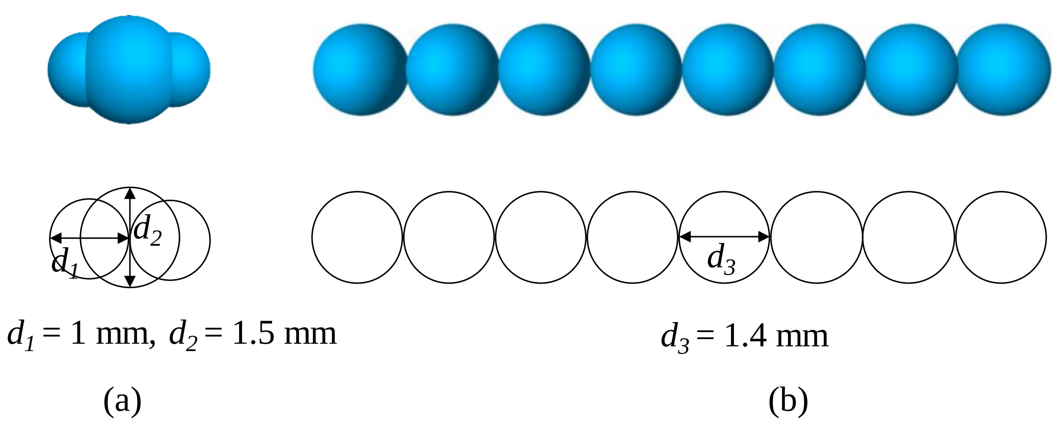

Fig. 2 Discrete element modeling of a sand particle and a rubber fiber: a) a sand particle with a diameter of 1.5 mm, and b) a rubber fiber with a diameter of 1.4 mm and a length of 11.2 mm

As illustrated in Fig. 3, a linear contact model and a parallel-bond contact model were adopted to define the interparticle and intraparticle interactions, respectively. Specifically, the linear contact model (Fig. 3(a)) was defined for the interparticle contacts of the sand–sand (SS), sand–rubber (SR) and rubber–rubber (RR). In this model, the contact stiffness is the harmonic average between the stiffnesses of two contacted particles, and the contact force has a linear correlation with the relative displacement between the contacted particles. Asadi et al. (2018a and 2018b) indicated that the Hertz model was the best choice to calculate the contact stiffness between the sand and rubber particles with large difference in stiffness. For the consideration of the compatibility with the parallel-bond model, the simple harmonic average for the contact stiffness was still adopted, but a more carful calibration was conducted to the error. Owning to the diverse material stiffness of the sand and rubber, the interparticle contact stiffness between SS, SR and RR particles were different, thereby resulting in various interparticle contact deformations. Besides, the contact-slip law was defined to determine the shear slip between the contacted particles along the tangential direction, in which the interparticle friction coefficient was the minimum friction coefficient of the contacted particles. For the intraparticle contacts inside a rubber cluster, the parallel-bond contact model was defined, which can be assumed as a certain thickness of cement with a tensile and shear strength, as demonstrated in Fig. 3(b). This model allowed for the modeling of compressive, tensile and bending deformation and the elastic springback of the rubber fiber under different loading conditions (Itasca, 2016). The validation and calibration of the DEM model and the mentioned parameters are discussed in section 3.

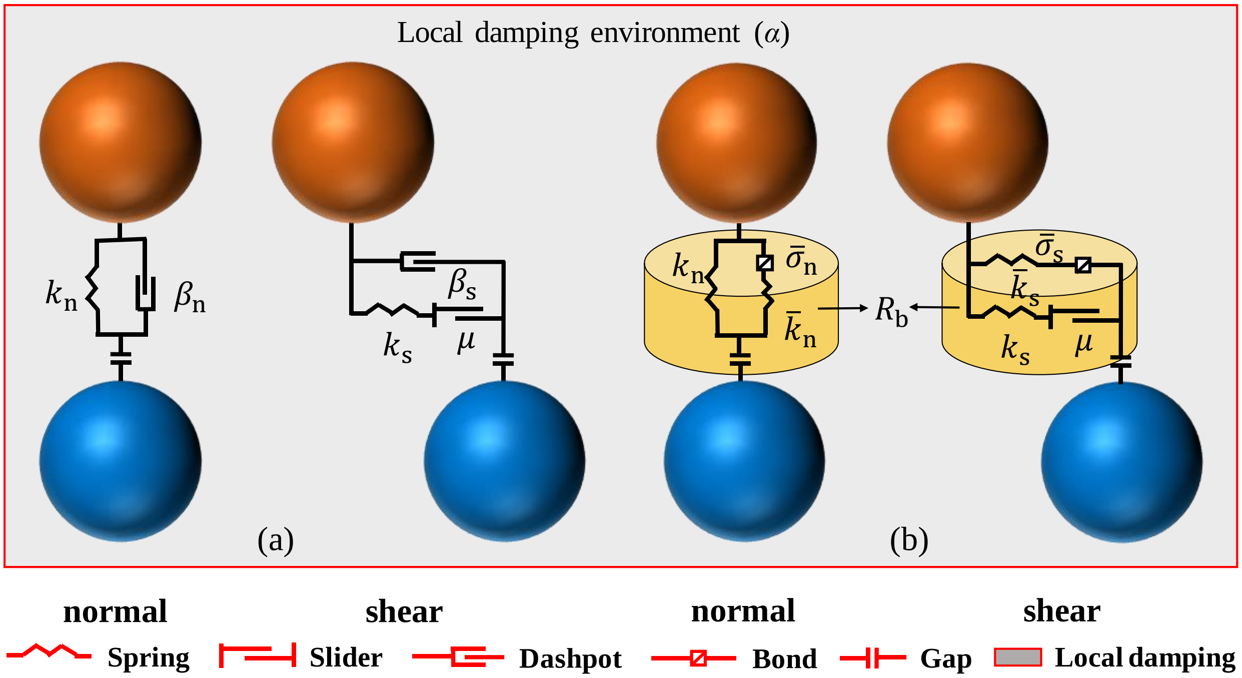

Fig. 3 Diagram of the adopted interparticle contact models: a) linear contact model, and b) parallel-bond contact model.

As the aim of this work was to investigate the effects of rubber fiber content on the macroscopic and microscopic mechanical behaviors of sand–rubber mixtures and to determine the optimum rubber content in terms of soil performance, rubber fiber contents of 10%, 20% and 30% by weight were selected to represent the range of contents commonly used to prepare these sand–rubber mixtures. To increase the computing efficiency of DEM simulations, the size of the triaxial samples was scaled to a diameter of 30 mm and a height of 60 mm. Within each sample, the sand particles were of a single grading, with a mean particle size of 1.5 mm, and the rubber fibers had a uniform length and diameter as in Fig. 2(b). To generate triaxial samples using the DEM, the initial void ratio was set to 0.55 for all of the samples. Therefore, the numbers of sand particles and rubber fibers within each sample were calculated according to their volume fraction.

Using an intrinsic function ‘clump template’ in the commercial DEM platform PFC^{3D} (Itasca, 2016), each sand–rubber mixture sample was created by randomly generating rigid clumps of the sand particle and rubber fiber inside a cylindrical boundary. The clump system was then solved to reach an initial equilibrium. Subsequently, all the clumps of the rubber fiber were released to deformable clusters with parallel-bonds. The servo-control mechanism was then utilized to reach the initial stress state of the sample with a given confining pressure. Figure 4 shows the generated DEM samples of pure sand and sand–rubber mixtures with various rubber contents. Figure 5 highlights the spatial distributions of the rubber fibers, accompanying with the polar distributions of the fiber orientation, inside the sand-rubber mixture samples. Overall, the sand particles and rubber fibers were uniformly distributed in the sample space, indicating good homogeneity of the generated samples. A slight anisotropy of the fiber orientation along the radial direction can be observed within the samples. It was reasonable that the fiber is more likely to rotate towards the vertical direction under compression. Based on the current DEM configuration, the time step of the system was approximately 2×10^{-7} s, and the average DEM computation time of the sand-rubber mixtures was approximately 19 h using 6 cores, each with a 3.2 GHz intel Core i7-8700 CPU.

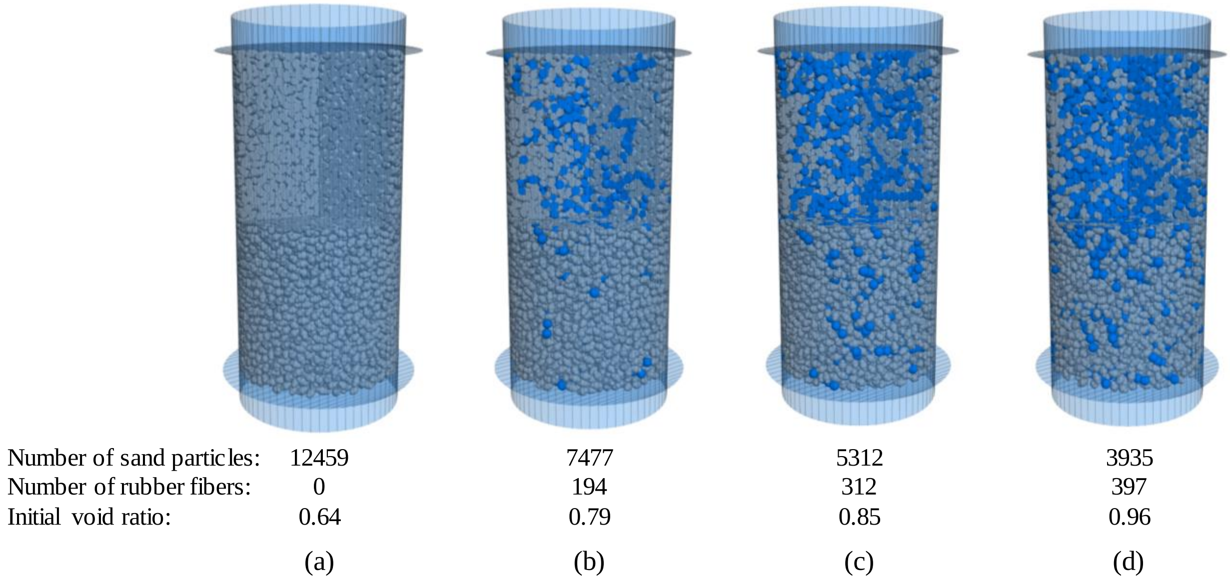

Fig. 4 DEM samples of pure sand and sand–rubber mixtures: a) pure sand, b) 10% rubber content, c) 20% rubber content, d) 30% rubber content

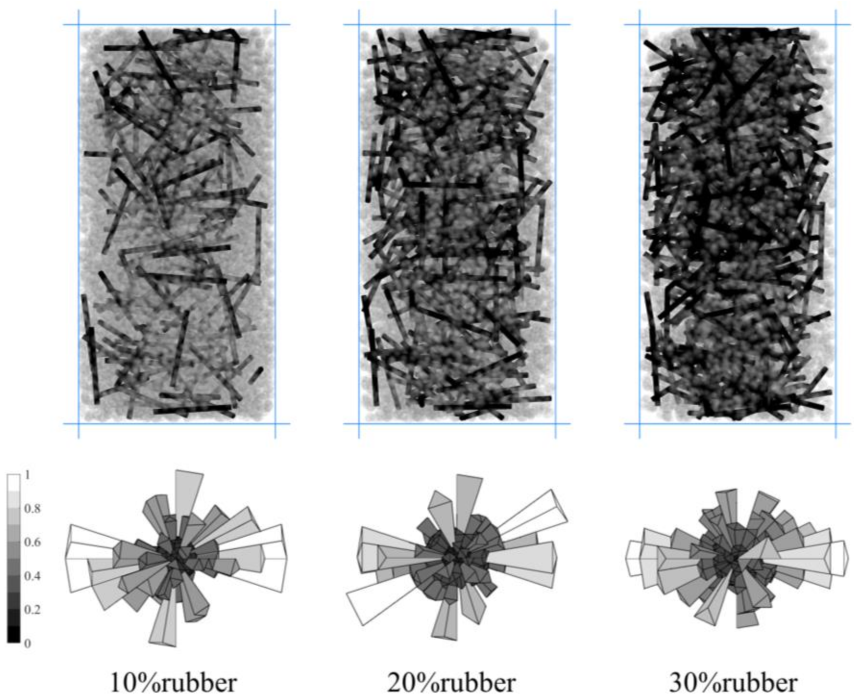

Fig. 5 Spatial distributions of the rubber fibers, accompanying with the polar distributions of the fiber orientation, inside the sand-rubber mixture samples

3 Calibration and validation

A conventional trial-and-error method based on comparisons between DEM simulations and real experiments was used to calibrate the DEM parameters. Briefly, the target mechanical behaviors identified in the DEM simulations were matched with those in the corresponding experiments to the maximum extent by continuously modifying the main controlling parameters in the DEM (Fu et al., 2017b; Coetzee, 2017). Specifically, for a rubber fiber cluster, the contact stiffness of the ball elements and the parallel-bond strength are the most important determinants of deformation and fracture properties (Itasca, 2016). Therefore, uniaxial tensile tests of a rubber fiber cluster (see Fig. 2(b)) were simulated and the results were compared with the experimental data. Fig. 6 shows the comparison of the data generated by the DEM simulation and experiment using the calibrated DEM parameters summarized in Table 1. By default, the local damping coefficient was set to 0.7, while the viscous coefficient was set to zero in the whole study, to guarantee the quasi-static modelling of DEM (Itasca, 2016). This figure shows good agreement between the numerical and experimental results, as both indicated an approximately linear relationship between tensile force and displacement at the earlier loading stage and a close failure point of the loading curve. Therefore, it was reasonable to use a line cluster of bonded ball elements and associated DEM parameters to simulate the rubber fibers.

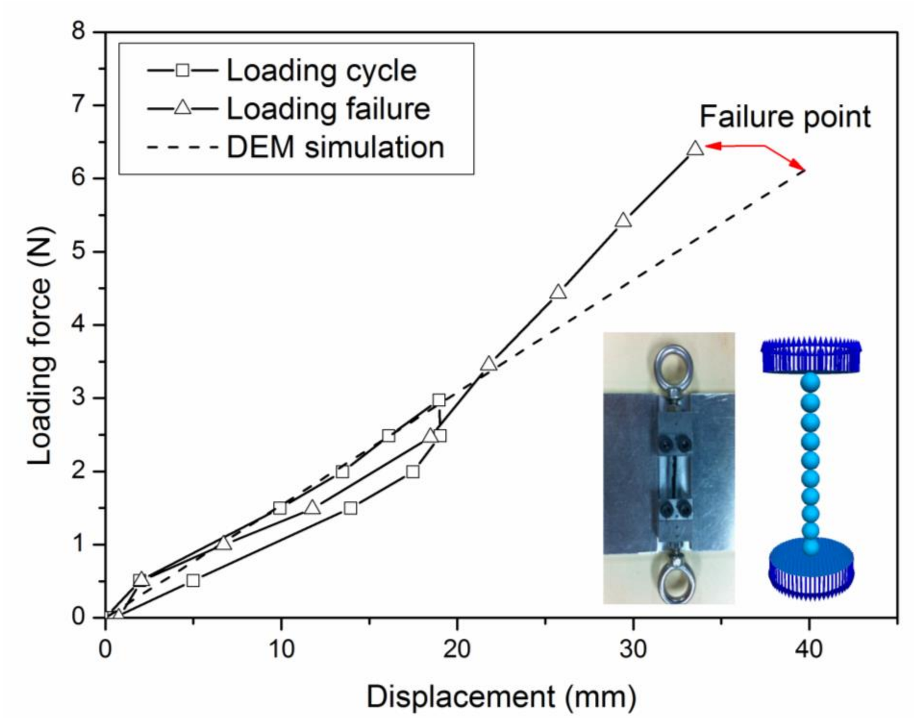

T

Fig. 6 Relationship between the loading force and displacement of the rubber fiber according to DEM and experimental results

Table 1 DEM parameters adopted in this study

Items	**Parameter**	**value**
Sand particle (ball element)	Density (kg/m^3)	2630
	Mean size (mm)	1.5
	Normal/shear stiffness (N/m)	5.0×10^6
	Interparticle friction coefficient	0.35
Rubber fiber (ball element and parallel-bond)	Density (kg/m^3)	1150
	Diameter and length (mm)	1.4, 11.2
	Normal/shear stiffness of ball elements (N/m)	2.5×10^4
	Interparticle friction coefficient of ball elements	0.6
	Normal/shear stiffness of parallel-bonds (N/m^3)	9×10^8
	Normal/shear strength of parallel-bonds (N/m^2)	4×10^6
	Ratio of bond radius to ball radius	1.0
Wall	Normal stiffness of top and bottom walls (N/m)	1×10^5
	Normal stiffness of cylindrical wall (N/m)	10^7
	Friction coefficient	0.0
System	Local damping coefficient	0.7
	Viscous damping coefficient	0

Initially, the pure sand samples were subjected to a set of triaxial tests to calibrate the DEM parameters for the sand particles. Figure 6 demonstrates the experimental and DEM findings corresponding to the macroscopic mechanical responses of pure sand samples subjected to triaxial compression under different confining pressures, using the DEM parameters summarized in Table 1. The comparison clearly indicated good agreement between the DEM results and the experimental results, especially for the relationship between the deviatoric stress and axial strain (Fig. 7(a)). The stress–strain curves generated from both the experimental and the DEM results exhibit obvious peak and strain-softening behaviors, which are highly consistent with the expected mechanics of pure sands. Regarding the relationship between volumetric strain and axial strain (Fig. 7(b)), a minor difference between the experimental and DEM results was observed at large strain stages, which might be due to the idealized particle shape and rigid servo boundary adopted in the DEM simulations. Kozicki et al. (2014) and Zhou et al. (2013) found that the irregular particle shape and rigid servo boundary tended to overestimate the volumetric strain of a sample within a DEM simulation compared with the regular particle shape and flexible servo boundary. Generally, the experimental and DEM results demonstrated a highly consistent tendency for shear-induced compression at pre-peak stress states and shear-induced dilation at post-peak stress states. Overall, the DEM and adopted DEM parameters were found to be capable of modeling the constitutive behavior of the pure sand sample.

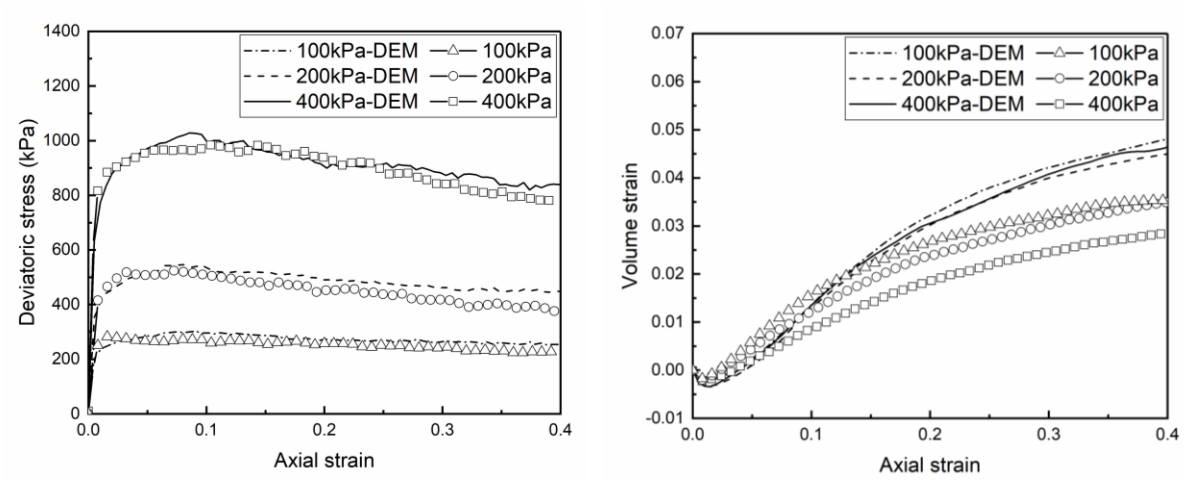

(a) (b)

Fig. 7 Comparative results of triaxial experiments and DEM simulations: a) deviatoric stress versus axial strain; b) volumetric strain versus axial strain (triaxial test data from Fu et al., 2017a)

Finally, triaxial testing on sand–rubber mixtures with a rubber contents of 10% and 30% were simulated to validate further the use of the DEM and adopted DEM parameters to simulate sand–rubber mixtures. Figures 8 and 9 show the mechanical response of the 10% and 30% mixtures subjected to triaxial compression under different confining pressures, based on the laboratory experiments and DEM simulations. Generally, comparative analysis of the results indicated that the mechanical behaviors determined from the DEM simulations agree well with those identified in the laboratory experiments, especially for the stress-strain curves of the10% mixture (Fig. 8(a)). Moreover, the relationship between volumetric strain and axial strain exhibited a consistent trend in both the experimental and the DEM results, especially for the 30% mixture (Fig. 9(b)). Conclusively, the proposed DEM model and adopted DEM parameters were shown to be robust and optimal for simulating the mechanical behaviors of sand–rubber mixtures.

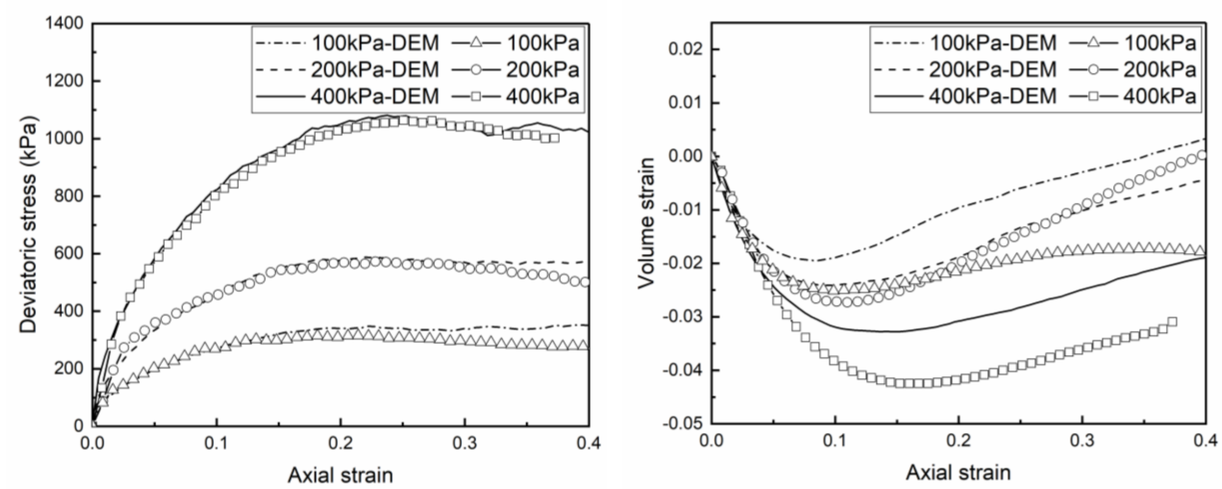

(a) (b)

Fig. 8 Comparative results of triaxial tests and DEM simulations of a 10% mixture: a) deviatoric stress versus axial strain, b) volumetric strain versus axial strain (triaxial test data from Fu et al., 2017a)

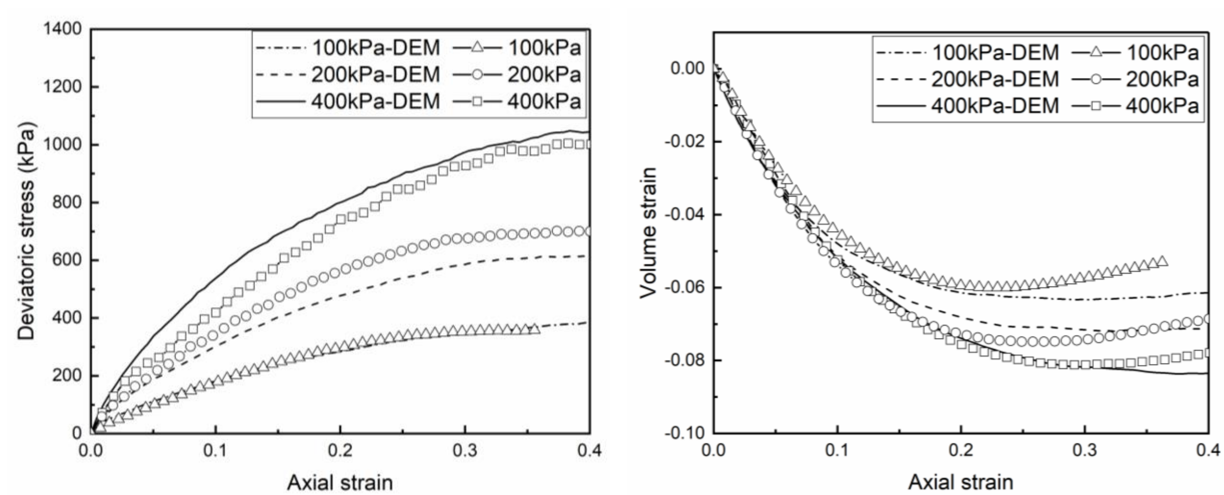

(a) (b)

Fig. 9 Comparative results of triaxial tests and DEM simulations of a 30% mixture: a) deviatoric stress versus axial strain, b) volumetric strain versus axial strain (triaxial test data from Fu et al., 2017a)

4 Results and discussion

4.1 Macroscopic mechanical behaviors

To investigate the effect of rubber content on the macroscopic and microscopic mechanical behaviors of sand–rubber mixtures, an additional DEM simulation was conducted on sand–rubber mixture samples with rubber content of 20%. Figure 10 shows the macroscopic mechanical responses of the sand–rubber mixtures subjected to triaxial compression under various confining pressures. Overall, the pure sand samples show a clear deviatoric stress peak and a strain-softening behavior post-peak until the critical state, whereas all of the sand–rubber mixture samples exhibited a continuous strain-hardening behavior at large strains until reaching the critical state, especially for the lowest confining pressure of 100 kPa (Fig. 10(a)). Correspondingly, the pure sand samples show a significant volumetric dilation post-peak until reaching the critical state, whereas all of the sand–rubber mixture samples exhibited continuous volumetric compression at large strains until reaching the final critical state.

Specifically, as the rubber content increased, the sand–rubber mixture samples tended to become increasingly compressible under shear stress. Accordingly, the stiffness pre-peak decreased significantly and the required axial strain to reach the peak deviatoric stress increased dramatically. These results agree well with the findings of the authors' previous experimental research (Fu et al., 2014 and 2017a). The high level of compressibility of the sand–rubber mixtures can be attributed mainly to the low level of material stiffness of the rubber fibers. Generally, rubber fibers appear to enhance the critical state shear resistance of a sand–rubber mixture. However, an increased rubber content seems to have limited improvement of the critical state shear resistance, especially under higher confining stresses (Fig. 10(c)). This inference was illustrated using the critical state data and the fitted lines in the spaces of deviatoric stress (q) and mean effective stress (p) plotted for all of the investigated samples, as shown in Fig. 11. The slope of the fitted critical state line (M) was used to better assess the reinforcing effect of rubber fibers in sand–rubber mixtures. Compared with the pure sand samples, the sand–rubber mixture samples yielded higher values of M, demonstrating the reinforcement effect of the rubber fibers. However, the values of M calculated for the sand–rubber mixture samples with rubber contents of 20% and 30% were extremely similar to each other, indicating that this increase in the rubber content did not significantly contribute to soil reinforcement. This finding agrees well with the experimental result obtained by Mashiri et al. (2015). Conclusively, given the observed reduction in soil stiffness, a rubber content of 20% is recommended to improve the mechanical performance of sand–rubber fiber mixtures.

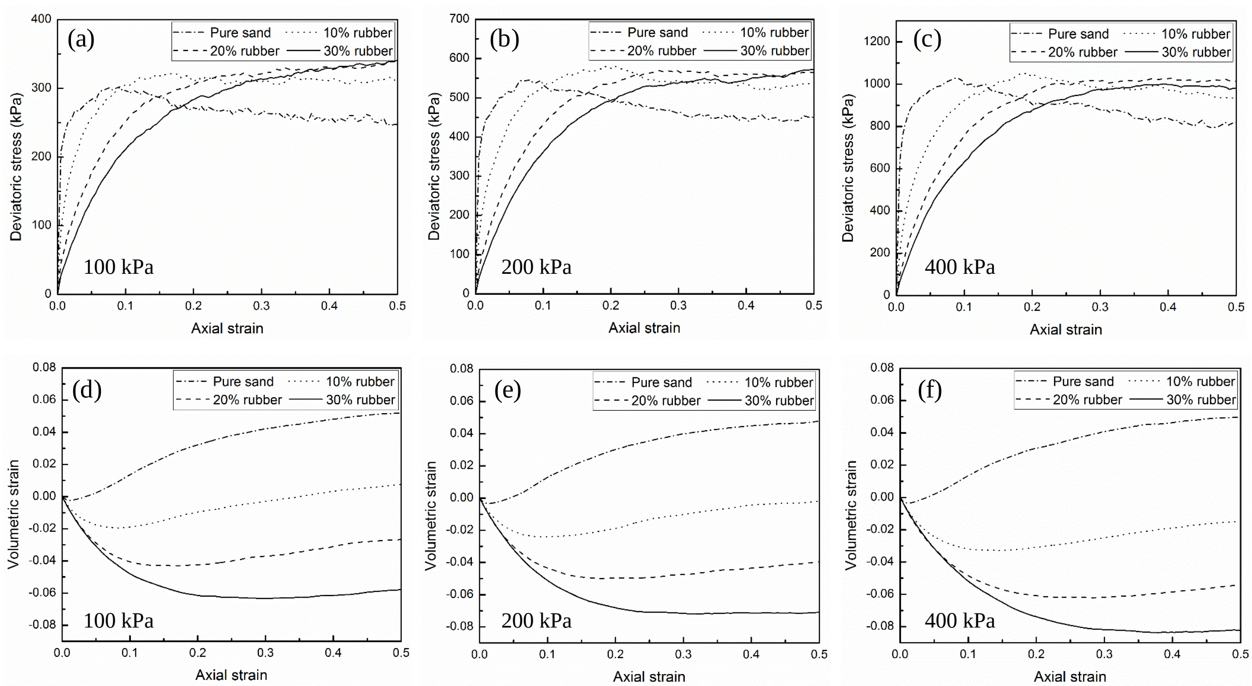

Fig. 10 Macroscopic mechanical behaviors of sand–rubber mixture samples subjected to triaxial compression under various confining pressures: a) – c) deviatoric stress versus axial strain for confining pressures of 100, 200 and 400 kPa; d) - f) volumetric strain for confining pressures of 100, 200 and 400 kPa

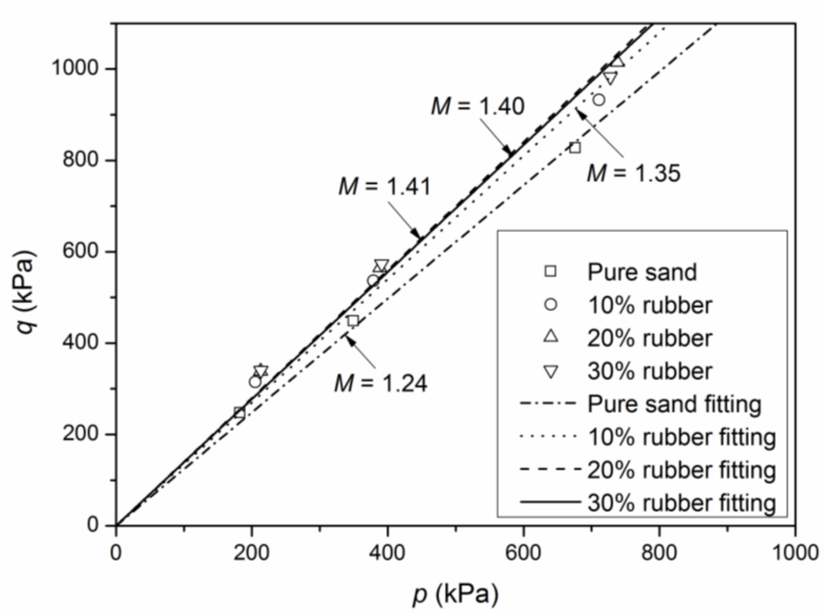

Fig. 11 Critical state data and fitted lines in *p*-*q* space for various sand–rubber mixtures

4.2 Microscopic mechanical behaviors

To understand the mechanism by which rubber fibers reinforce a sand–rubber mixture, micromechanical features, namely particle kinematics, the interparticle coordination number and rubber fiber deformation, were investigated and are discussed in this section.

Within the DEM model, the data for particle kinematics, in terms of particle displacements and rotations, are extracted to highlight shear banding since these are regarded as important indicators revealing local shear failure mechanisms of granular materials (Zhou et al. 2013; Wu et al., 2020). Figures 12 and 13 respectively demonstrate the evolution of the particle displacements and particle rotations of different samples as shearing developed. For both, a distinct localization phenomenon was observed within the pure sand sample post-peak (Figs. 12(a) and 13(a)). This phenomenon became less apparent within the sand–rubber mixture samples as the rubber content increased, even at extremely large strains (Figs. 12(d) and 13(d)). This finding agrees well with the experimental results generated from a mini sand–rubber mixture samples subjected to triaxial compression and observed using in-situ X-ray CT scanning (Cheng et al., 2020b). The failure pattern of the sand–rubber mixture gradually shifts from a local shear failure to an overall shear failure as the rubber content increases. This reveals an essential reinforcing mechanism of rubber fibers within a sand–rubber mixture, which can be considered a hysteresis effect that restrains the development of local shear failure.

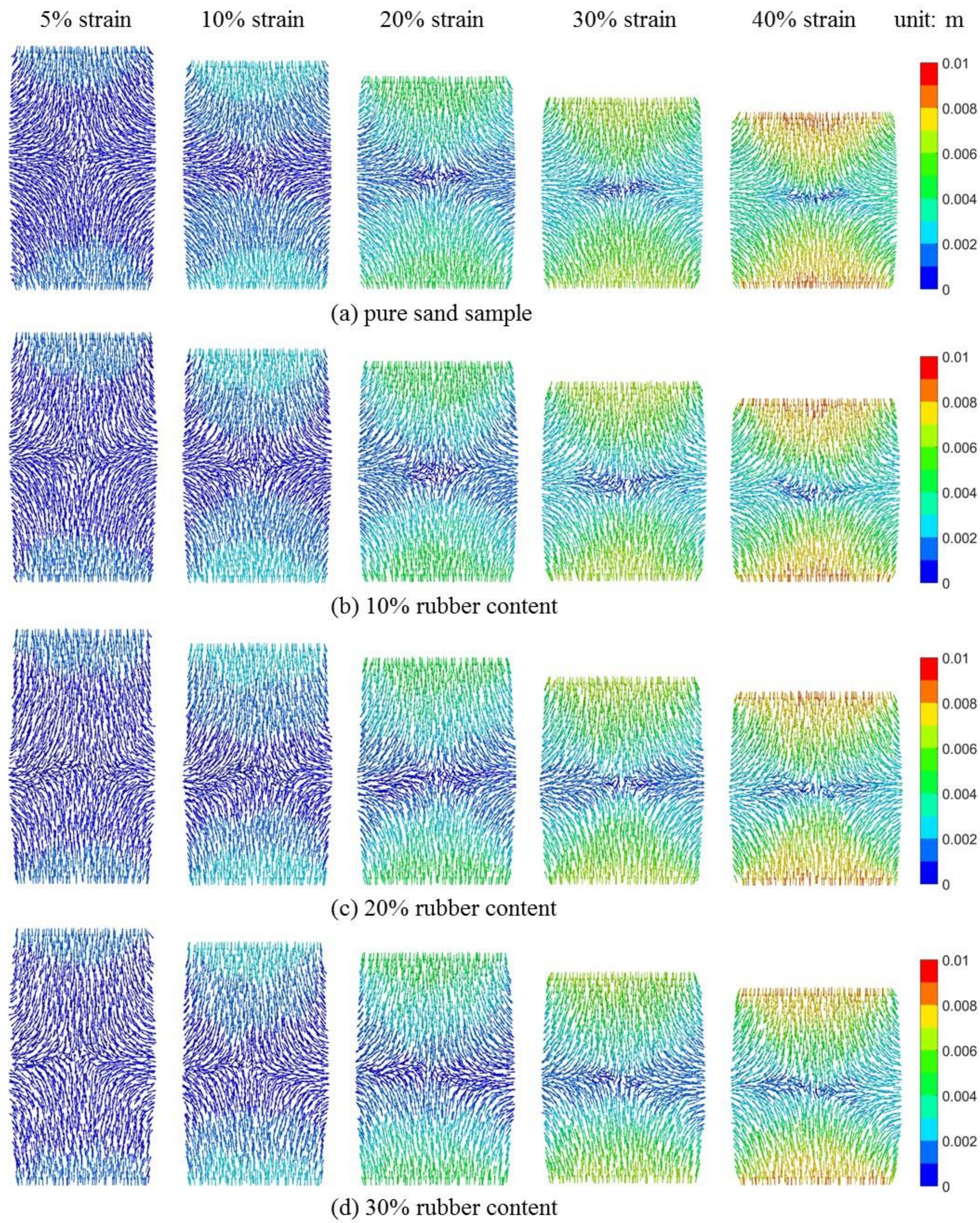

Fig. 12 Particle displacement fields within the vertical sections through the middle of the samples: a) pure sand sample; sand–rubber mixture samples with rubber contents of b) 10%, c) 20% and d) 30%

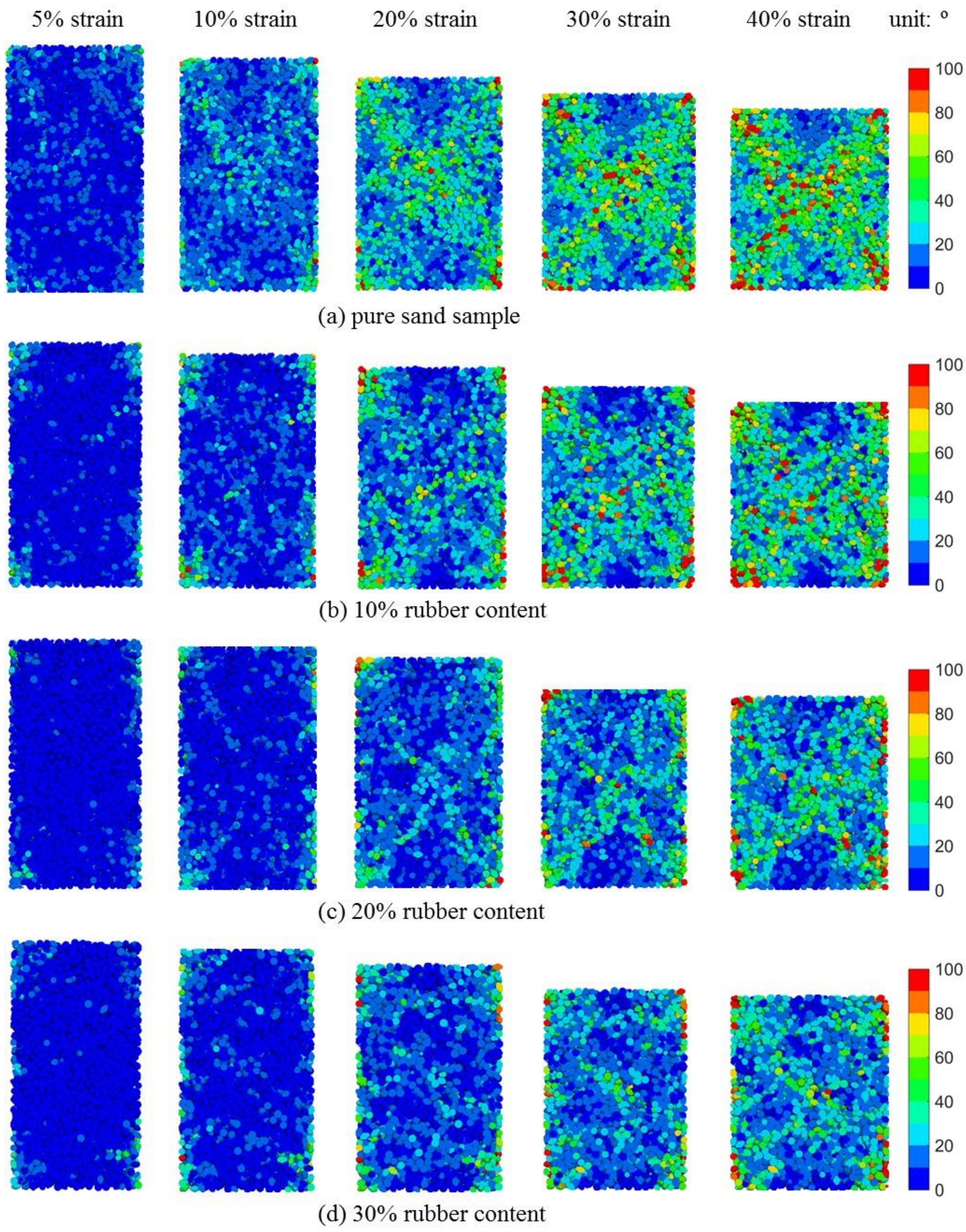

Fig. 13 Particle rotation fields within the vertical sections through the middle of the samples: a) pure sand sample; sand–rubber mixture samples with rubber contents of b) 10%, c) 20% and d) 30%

To investigate the interparticle coordination number within the sand–rubber mixtures, the overall interparticle contacts and interparticle contacts between sand particles were targeted, mainly because these are the predominant components of the bearing structure of a particle system. The interparticle coordination number was defined by the total contacts between the comprised ball elements of the contacted particles. Figure 14 shows the development of the mean coordination number of these two types of interparticle contacts within samples subjected to triaxial compression under different confining pressures. Interestingly, in the pure sand sample, the mean coordination number remained approximately constant throughout the shearing process. In contrast, in the sand–rubber mixture samples, the mean coordination number of the overall interparticle contacts gradually increased during the shearing process (Figs. 14(a) – 14(c)), and the mean coordination number of the sand–sand interparticle contacts initially increased and then slightly decreased as shearing developed (Figs. 14(d) – 14(f)). The volumetric compression of the sand–rubber mixtures contributed to the continuous increase of the coordination number of the overall interparticle contacts within the sample. For the sand–sand interparticle contacts within the sand–rubber mixture samples, the early volumetric compression enhanced the coordination number; however, the deformed rubber was more likely to fill the interparticle voids between the sand particles, thereby decreasing the coordination number between the sand particles at large strains.

For all of the samples at any certain shearing strain level, with increasing rubber content, the mean coordination number of the overall interparticle contacts increased significantly, whereas the mean coordination number of the sand–sand interparticle contacts decreased. Here, the increased rubber content significantly enhanced the overall interparticle contacts but simultaneously weakened the sand–sand interparticle contacts. As the sand–sand interparticle contacts play a major role in constructing the bearing structure of the particle system, whereas the sand–rubber and rubber-rubber interparticle contacts play only minor roles, the increased coordination number of the overall interparticle contacts and the decreased coordination number of the sand–sand interparticle contacts may indicate that the reinforcing effect of increased rubber content was compromised. This result provides an essential insight into the limited reinforcing quality of a sand–rubber mixture with a very high rubber contents.

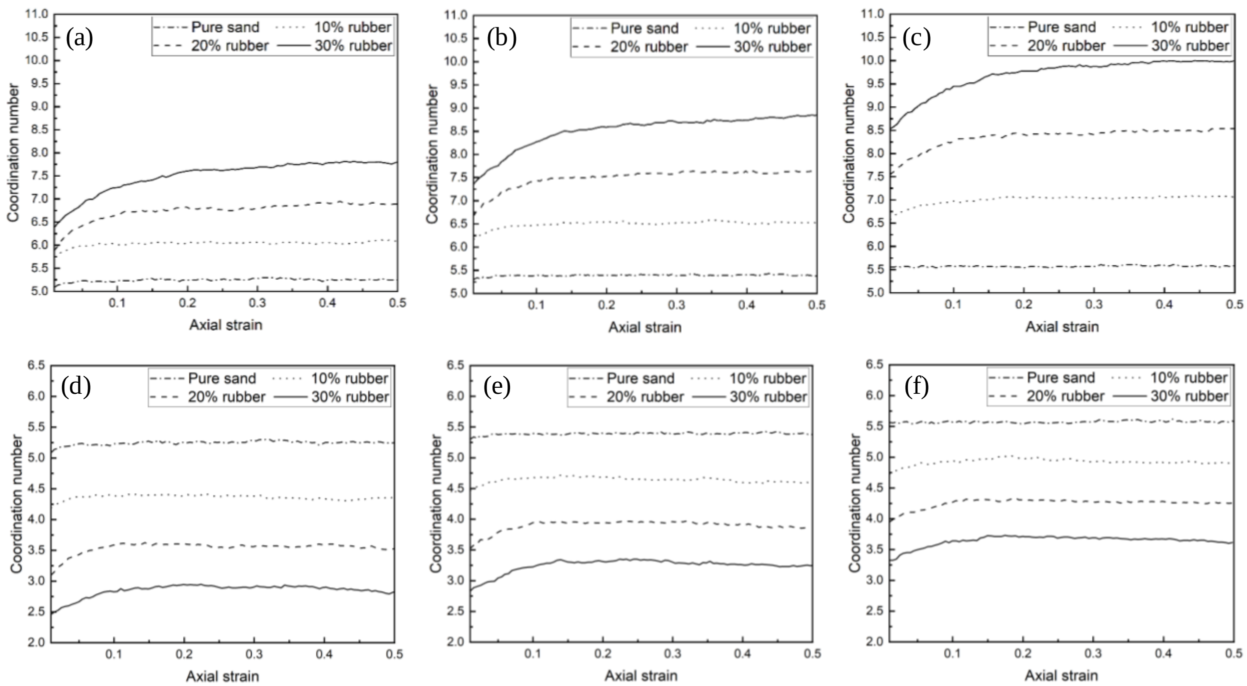

Fig. 14 Development of the mean coordination numbers of two types of interparticle contacts: a) – c) overall interparticle contacts under confining pressures of 100, 200 and 400 kPa; d) – f) sand–sand interparticle contacts under confining pressures of 100, 200 and 400 kPa.

Because rubber is an easily deformed material, it was also important to investigate the deformation behaviors of rubber fibers within sand–rubber mixtures to gain novel insights into the reinforcing mechanisms of the rubber fibers. The ratio of the length of a deformed rubber fiber (I) to its original length (I_0) was defined to characterize the degree of deformation of the rubber fiber. A rubber fiber is compressed when I/I_0 is less than 1.0 and stretched when I/I_0 is greater than 1.0. Figure 15 shows the development of the average length ratio of all of the rubber fibers within a sand–rubber mixture under different confining pressures. The rubber fibers in the observed mixtures were slightly compressed in the initial shearing stages and clearly stretched at large strains. The axial strains at which the rubber fibers transformed from general compression to general stretching tended to increase as the confining pressure increased.

An important observation is that the average length ratio of the rubber fibers significantly increased with decreasing rubber content, especially for the sample under the highest confining pressure (Fig. 15(c)). This indicates that the rubber fibers inside the sand–rubber mixture with a lowest rubber content are more likely to stretch than when there is a higher rubber content. This finding was illustrated by the probability density function (PDF) of the length ratios of all of the rubber fibers within the various sand–rubber mixtures at the critical state in Fig. 16. In Fig. 16(c), the value of the length ratio at the peak of the PDF curve is much greater for the sand–rubber mixture with 10% rubber content (approximately 1.2) than for the mixture with 30% rubber content (approximately 1.06). These findings reveal a crucial micromechanism of soil reinforcement that relies on the deformation of rubber fibers. Compared with a sand–rubber mixture with a higher rubber content, a mixture with a lower rubber content will exhibit better rubber fiber deformation and thus better resist local shear failure. The results again indicate that 20% is the optimum rubber content with respect to the mechanical performance of a sand–rubber mixture.

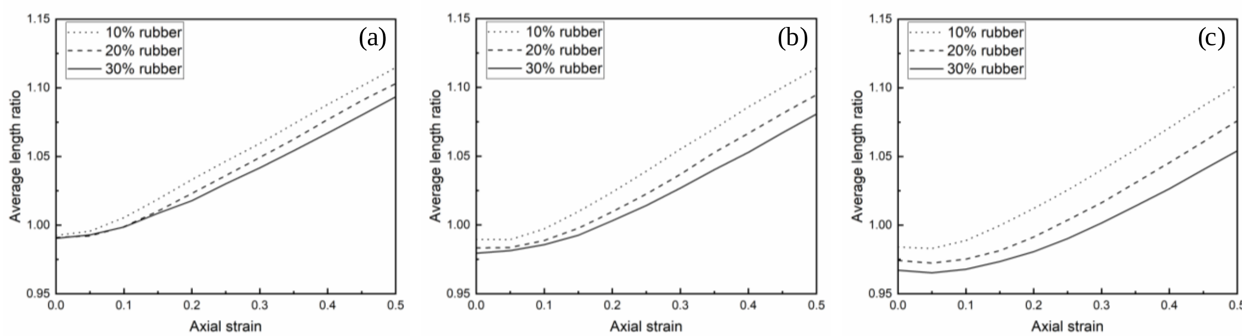

Fig. 15 Development of the average length ratios of the rubber fibers within various sand–rubber mixtures under confining pressures of a) 100 kPa, b) 200 kPa and c) 400 kPa

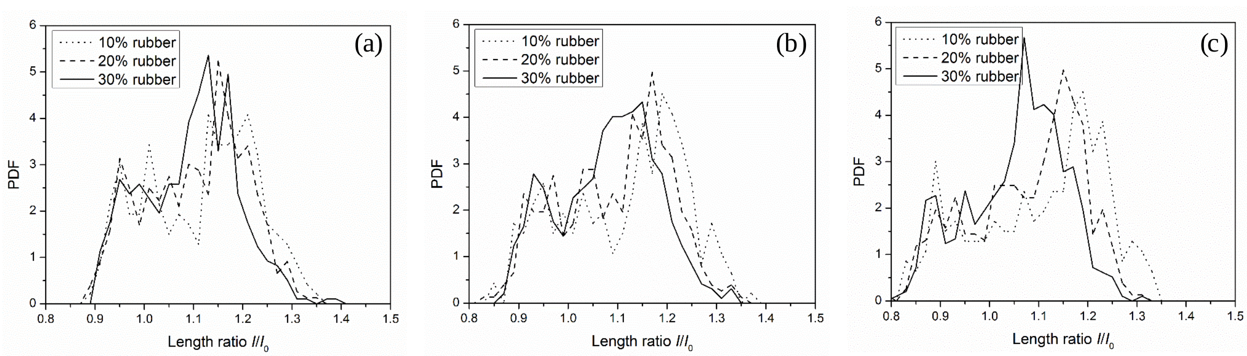

Fig. 16 Probability density function of the deformation ratios of all of the rubber fibers within various sand–rubber mixture samples in the critical state under confining pressures of a) 100 kPa, b) 200 kPa and c) 400 kPa

5 Conclusion

In this study, a series of DEM simulations and calibrations of granular soils with tire rubber fibers were conducted, and the effect of rubber content on the macroscopic and microscopic behaviors of the sand-rubber mixtures was investigated. The specific reinforcing mechanism of rubber fibers within a sand–rubber mixtures was revealed by analyzing particle micromechanics and used to determine the optimum rubber content. The following major conclusions can be drawn.

(1) Within the DEM model, a rigid clump and a deformed cluster with parallel-bonded interparticle contacts can be used to model the mechanics of granular soils and tire rubber

fibers with small tensile deformation, respectively. Based on a comparative study of the experimental and DEM results, the proposed DEM method and adopted DEM parameters were shown to provide a robust and accurate simulation of the mechanical behaviors of a sand–rubber mixtures subjected to triaxial compression.

(2) Both the experimental and the DEM results indicate that the rubber fibers had a significant reinforcing effect on the shear resistance of the sand–rubber mixtures at the critical state. However, increasing the rubber content from 20% to 30% resulted in only a limited improvement of the shear resistance. The sand–rubber mixtures tended to become increasingly compressible in shear at higher rubber contents, resulting in a continuous decrease of stiffness pre-peak. Therefore, a sand–rubber mixture with a rubber content of 20% is recommended to give the best mechanical performance. This finding was consistent with the experimental result by Mashiri et al. (2015), who found the sand-rubber mixture with 20% tire chips has the largest shear strength.

(3) The addition of rubber fibers produced a hysteresis effect restraining the development of local shear failure in the sand–rubber mixtures. However, due to the large deformations of rubber fibers, increasing the rubber content significantly enhanced the overall interparticle contacts but weakened the sand–sand interparticle contacts within the mixtures. Moreover, rubber fibers in the mixture with a lower rubber content are more likely to be stretched, indicating that rubber fibers show better deformation performance and greater shear failure resistance at a lower rubber content. The particle micromechanics data generated in this study provide an understanding of reinforcing mechanism of rubber fibers within a sand–rubber mixture and conclusive evidence of the rubber content required to optimize soil performance.

Due to the limitation of the idealized particle shapes by conventional modelling techniques, the future work will develop a more detailed DEM method to simulate the real morphologies of rigid sand particles and deformed rubber fibers. Moreover, to verify the obtained micromechanics from DEM, the in-situ experiment on sand-rubber mixtures subjected to X-ray micro-CT scanning will be conducted along this research line.

Acknowledgments

This study was supported by Research Grants Nos. 42277169, and No. 4202010400 from the National Science Foundation of China. The authors are grateful for the contributions of the reviewers.

References

Abbaspour, M., Narani, S.S., Aflaki, E., Moghadas Nejad, F., and Mir Mohammad Hosseini, S.M., 2020. Strength and swelling properties of a waste tire textile fiber-reinforced expansive soil. Geosynth. Int., 27(5), 476-489.

Ahn, I.S., and Cheng, L., 2014. Tire derived aggregate for retaining wall backfill under earthquake loading. Constr. Build. Mater., 57, 105-116.

Akbulut, S., Arasan, S., Kalkan, E. 2007. Modification of clayey soils using scrap tire rubber and synthetic fibers. Appl. Clay Sci., 38: 23-32.

Al-Rkaby, A., 2019. Strength and Deformation of Sand-Tire Rubber Mixtures (STRM): An Experimental Study, Studia Geotech. et Mech., 41(2), 74-80.

Anbazhagan, P., Manohar, D.R., and Rohit, D., 2017. Influence of size of granulated rubber and tyre chips on the shear strength characteristics of sand–rubber mix. Geomech. Geoeng., 12(4), 266-278.

Asadi, M., Mahboubi, A., & Thoeni, K., 2018a. Discrete modeling of sand–tire mixture considering grain-scale deformability. Granul. Matter, 20(2), 1-13.

Asadi M, Mahboubi A., Thoeni K. Towards more realistic modelling of sand–rubber mixtures considering shape, deformability, and micro-mechanics. Can. Geotech. J. 2023, 60(2): 182-197.

Asadi M., Thoeni K., & Mahboubi A., 2018b. An experimental and numerical study on the compressive behavior of sand-rubber particle mixtures. Comput. Geotech., 104: 185-195.

ASTM., 2008. Standard practice for use of scrap tires in civil engineering applications. D6270, West Conshohocken, PA.

Attom M.F., 2006. The use of shredded waste tires to improve the geotechnical engineering properties of sands. Environ. Geol., 49(4): 497-503.

Balaban, E., Smejda, A., and Onur, M.I., 2019. Influence of tire crumbs on mechanical properties of sand-fine soil mixtures. Geomech. Geoeng., 1-16.

Batayneh, M.K., Marie, I., & Asi, I., 2008. Promoting the use of crumb rubber concrete in developing countries. Waste Manage., 28(11), 2171-2176.

Bekhiti, M., Trouzine, H., Rabehi, M., 2019. Influence of waste tire rubber fibers on swelling behavior, unconfined compressive strength and ductility of cement stabilized bentonite clay soil, Constr. Build. Mater., 208, 304-313.

Benessalah, I., Arab, A., Sadek, M., and Bouferra, R., 2019. Laboratory study on the compressibility of sand–rubber mixtures under one dimensional consolidation loading conditions. Granul. Matter, 21(1), 1-9.

Cabalar, A.F., 2011. Direct shear tests on waste tires–sand mixtures. Geotech. Geol. Eng., 29(4), 411-418.

Cetin, H., Fener, M., Gunaydin, O., 2006. Geotechnical properties of tire-cohesive clayey soil mixtures as a fill material, Eng. Geol., 88(1-2), 110-120.

Cheng, Q., Tang, C.S., Chen, Z.G., El-Maarry, M.R., Zeng, H., and Shi, B., 2020a. Tensile behavior of clayey soils during desiccation cracking process. Eng. Geol., 279, 105909.

Cheng, Z., Wang, J. and Li, W., 2020b. The micro-mechanical behaviour of sand–rubber mixtures under shear: An experimental study based on X-ray micro-tomography. Soils Found., 60(5), 1251-1268.

Chew, K., Chiaro, G., Vinod, J. S., Tasalloti, A., and Allulakshmi, K. 2022. Direct shear behavior of gravel-rubber mixtures: Discrete element modeling and microscopic investigations. Soils Found., 62(3): 101156.

Coetzee, C. J., 2017. Calibration of the discrete element method. Powder Technol., 310, 104-142.

Consoli, N., Prietto, P., Montardo, J., and Pasa, G., 2002. Engineering behavior of a sand reinforced with plastic waste. J. Geotech. Geoenviron. Eng., 128 (6), 462-472.

Edincliler, A., Baykal, G. and Saygili, A., 2010. Influence of different processing techniques on the mechanical properties of used tires in embankment construction. Waste Manage., 30, 1073-1080.

Fu, R., Coop, M.R., Li, X.Q., 2014. The mechanics of a compressive sand mixed with tire rubber. Geotechnique Lett. 4 (3), 238-243.

Fu, R., Coop, M.R., Li, X.Q., 2017a. Influence of particle type on the mechanics of sand-rubber mixtures. J. Geotech. Geoenviron. Eng., 143, 1-15.

Fu, R., Hu, X., and Zhou, B., 2017b. Discrete element modeling of crushable sands considering realistic particle shape effect. Comput. Geotech., 91, 179-191.

Fu, R., Baudet, B.A., Madhusudhan, B.N., and Coop, M.R., 2018. A comparison of the performances of polypropylene and rubber fibers in completely decomposed granite. Geotext. Geomembr., 46(1), 22-28.

Gong, L., Nie, L., Liu, C., and Xu, Y., 2020. Modelling Triaxial Tests on Fibre-Reinforced Sands with Different Fibre Orientations Using the Discrete Element Method, KSCE J. Civ. Eng., 24(8), 2268-2280

Humphrey D N. Tire derived aggregate as lightweight fill for embankments and retaining walls. 2007. Proceedings International Workshop on Scrap Tire Derived Geomaterials, Yokosuka, Japan. 59-81.

Itasca C., 2016. PFC 3D Manual, Version 5.0. Itasca Consulting Group, Minneapolis.

Jiang, M., Yang, Z., Barreto, D., and Xie, Y., 2018. The influence of particle-size distribution on critical state behavior of spherical and non-spherical particle assemblies. Granul. Matter, 20(4), 1-15.

Kalkan E. 2013. Preparation of scrap tire rubber fiber-silica fume mixtures for modification of clayey soils, Appl. Clay Sci., 80-81, 117-125.

Kawata, S., Hyodo, M., Orense, R.P., Yamada, S. and Hazarika, H. 2008. Undrained and drained shear behavior of sand and tire chips composite material. Proceedings of the International Workshop on Scrap Tire Derived Geomaterials - Opportunities and Challenges, IW-TDGM 2007, 277-283.

Kozicki J., Tejchman J., Mühlhaus H.B., 2014. Discrete simulations of a triaxial compression test for sand by DEM. Int. J. Numer. Anal. Met. 38(18), 1923-1952.

Lee, C., Shin, H., Lee, J.S., 2014. Behavior of sand-rubber particle mixtures: experimental observations and numerical simulations. Int. J. Numer. Anal. Methods Geomech. 38 (16), 1651-1663.

Liu, F., Chen, G., Li, L. and Guo, Y., 2012. Study of impact performance of rubber reinforced concrete. Constr. Build. Mater., 36, 604-616.

Lopera Perez, J.C., Kwok, C.Y., Senetakis, K., 2016. Effect of rubber size on the behaviour of sand-rubber mixtures: a numerical investigation. Comput. Geotech. 80, 199-214.

Lopera Perez, J. C., Kwok, C.Y., Senetakis, K. 2017. Micromechanical analyses of the effect of rubber size and content on sand-rubber mixtures at the critical state, Geotext. Geomembr., 45(2), 81-97.

Lopera Perez, J. C., Kwok, C. Y., Senetakis, K. 2018. Effect of rubber content on the unstable behaviour of sand–rubber mixtures under static loading: a micro-mechanical study. Géotechnique, 68(7), 561-574.

Mashiri, M.S., Vinod, J.S., Sheikh, M.N. and Tsang, H.H., 2015. Shear strength and dilatancy behaviour of sand–tyre chip mixtures. Soils Found., 55(3), 517-528.

Moghaddas Tafreshi, S. N., Khalaj, O., and Dawson, A.R., 2013. Pilot-scale load tests of a combined multilayered geocell and rubber-reinforced foundation. Geosynth. Int., 20(3), 143-161.

Moghaddas Tafreshi, S. N., Joz Darabi, N., Tavakoli Mehrjardi, G., Dawson, A., 2019. Experimental and numerical investigation of footing behaviour on multi-layered rubber-reinforced soil. Eur. J. Environ. Civ. Eng., 23(1), 29-52.

Narani, S.S., Abbaspour, M., Hosseini, S. M.M., Aflaki, E., & Nejad, F.M., 2020. Sustainable reuse of Waste Tire Textile Fibers (WTTFs) as reinforcement materials for expansive soils: With a special focus on landfill liners/covers. J. Clean. Prod., 247, 119151.

Noorzad, R., and Raveshi, M., 2017. Mechanical behavior of waste tire crumbs–sand mixtures determined by triaxial tests. Geotech. Geol. Eng., 35(4), 1793-1802.

Reddy, S.B. and Krishna, A.M., 2015. Recycled tire chips mixed with sand as lightweight backfill material in retaining wall applications: an experimental investigation. Int. J. Geosynth. Ground. Eng., 1(4), 1-11.

Santos, A., Consoli, N., Baudet, B., 2010. The mechanics of fibre-reinforced sand. Géotechnique, 60(10), 791-799.

Shekhawat, P., Shrivastava, N., Shrivastava, S., 2018. Experimental Investigation on Durability of Soil Reinforced with Sustainable Fibers Subjected to Wet-Dry Cycles. Urbanization Challenges in Emerging Economies: Resilience and Sustainability of Infrastructure: 234-243.

Soleimanbeigi, A., and Edil, T.B., 2015. Compressibility of recycled materials for use as highway embankment fill. J. Geotech. Geoenviron. Eng., 141(5), 04015011.

Soltani, A., Deng, A., Taheri, A., & Sridharan, A., 2018. Swell–shrink–consolidation behavior of rubber–reinforced expansive soils. Geotechnical Testing Journal, 42(3), 761-788.

Tasalloti, A., Chiaro, G., Murali, A., & Banasiak, L., 2021. Physical and mechanical properties of granulated rubber mixed with granular soils—a literature review. Sustainability, 13(8), 4309.

Thomas B.S. and Gupta R.C., 2016. Properties of high strength concrete containing scrap tire rubber. J. Clean. Prod., 113: 86-92.

Trouzine, H., Bekhiti, M., & Asroun, A., 2012. Effects of scrap tyre rubber fibre on swelling behaviour of two clayey soils in Algeria. Geosynth. Int., 19(2), 124-132.

Valdes, J.R., Evans, T.M., 2008. Sand-rubber mixtures: Experiments and numerical simulations. Can. Geotech. J. 45 (4), 588-595.

Wu, M., Wang, J., Russell, A., & Cheng, Z., 2020. DEM modelling of mini-triaxial test based on one-to-one mapping of sand particles. Géotechnique, 1-14.

Wu, Q., Xu, T., and Yang, Z., 2020. Diffuse instability of granular material under various drainage conditions: discrete element simulation and constitutive modeling. Acta Geotech., 15(7), 1763-1778.

Yang, Z., Wu, Y., 2017 Critical state for anisotropic granular materials: a discrete element perspective. Int. J. Geomech., 2, 04016054.

Yoon, S., Prezzi, M., Siddiki, N. Z. and Kim, B. 2006. Contruction of a test embankment using a sand-tire shred mixture as fill material. Waste Manage., 26: 1033-1044.

Zhang J., Chen X., Zhang J., Jitsangiam, P., & Wang, X., 2021. DEM investigation of macro-and micro-mechanical properties of rigid-grain and soft-chip mixtures. Particuology, 55: 128-139.

Zhou, B., Huang, R., Wang, H., and Wang, J., 2013. DEM investigation of particle anti-rotation effects on the micromechanical response of granular materials. Granul. Matter, 15(3), 315-326.